Influence of spot size on propagation dynamics of laser-produced tin plasma

S. S. Harilal[a)]
Center for Energy Research, University of California San Diego, La Jolla, California 92093, USA

(Received 18 June 2007; accepted 21 October 2007; published online 20 December 2007)

The plume dynamics in the presence of an ambient gas is very intriguing physics. The expansion of a laser-produced plasma in the presence of an ambient gas leads to internal plume structures, plume splitting, sharpening, confinement, etc. We investigated propagation dynamics of an expanding tin plume for various spot sizes using a fast visible plume imaging and Faraday cup diagnostic tools. Our results indicate that the sharpening of the plume depends strongly on the spot size. With a smaller spot size, the lateral expansion is found to be higher and the plume expansion is spherical while with a larger spot size the plume expansion is more cylindrical. Analysis of time resolved imaging also showed internal structures inside the plume. © *2007 American Institute of Physics*. [DOI: 10.1063/1.2822450]

I. INTRODUCTION

The propagation dynamics of a plume is very important for most of the applications of laser-produced plasmas (LPP) including the extreme ultraviolet (EUV) lithography source,[1–4] pulsed laser deposition process,[5] nanocluster formation,[6,7] etc. The plume expansion in vacuum can be described as self-similar and adiabatic and is treated well by Anisimov *et al.*[8] Compared to plume expansion in vacuum; the interaction of the plume with an ambient gas is a far more complex gas dynamic process that involves deceleration, attenuation, and thermalization of the ablated species, as well as the formation of shock waves.[9–12] Our previous studies revealed a complex plume splitting in a laser created aluminum plasma expanding into an ambient environment where gas phase collisions transformed the initial temporal distribution into a very different final distribution.[12] We distinguished three distinct pressure regimes using fast photography, each of which is characterized by particular behavior of the plume. At low pressure or in vacuum, the plume expands freely without any external viscous force. At intermediate pressure levels (transition regime), the plume is characterized by strong interpenetration of the plasma species and background gas that leads to plume splitting and sharpening. At these pressure levels, a shock wave will be formed in the interface between the plume and background gas and a point blast model can be applied. At still high pressures, due to enhanced collisions with the background gas species, the deceleration process is very rapid and eventually plume propagation stops and particles become thermalized.[10] Apart from ambient gas, the dynamics of the plume is also influenced by other experimental factors like, focal spot size and shape, laser pulse width, irradiance, wavelength, etc.

The plume splitting and sharpening phenomena are described well in the literature.[5,10,13,14] In the transition regime a part of the plume penetrated into the ambient gas with vacuum-like expansion and another division of the plume species decelerated after interaction with ambient gas that lead to plume splitting. The plume splitting phenomenon was first observed by Geohegan[5] in laser produced $YBa_2Cu_3O_7$ plasma expansion into oxygen ambient and later Wood *et al.*[14] explained these phenomena based on a combination of multiple elastic scattering and hydrodynamic formulations. In spite of extensive work done on this topic, the propagation dynamics of LPP is not well understood and explained.

Laser-produced Sn plasma is a most promising candidate for next generation EUV lithographic light source.[1,2,15,16] Presently, a lot of efforts are going on worldwide for optimizing EUV emission from tin plasma and mitigating various debris coming from the plasmas. The debris includes fast ions and neutrals, clusters, and out of band emission and, hence, controlling the expanding plume species is indeed a greatest challenge for future LPP EUV light source. We employed various methods for controlling and/or mitigating energetic ions including; low-density targets,[4,17] ambient gas,[16] magnetic field,[18] pre-pulse[2] and synergetic effects (combination of two methods).[16] We recently reported that the spot size has negligible effect on the conversion efficiency (CE) of in-band radiation (13.5 nm with 2% bandwidth).[19] The constant CE irrespective of the spot size is attributed to the balance of the laser energy loss due to lateral expansion of the plasma and reabsorption of the EUV light.

The objective of this study is to understand the expansion dynamics of the laser produced tin plume with varying spot sizes. Fast photography and a Faraday cup ion detector are used for diagnosing the plume. Since the plume expands freely in vacuum, it may be difficult to understand the propagation dynamics of the plume with different spot sizes using fast photography in the visible region.[10,20] Hence, we inserted a low-pressure ambient gas to make the plume more collisional. The presence of low pressure ambient gas will lead to the formation of shock waves in the plume front and they are very useful for understanding the nature of the expansion. Our fast photography images show that the spot size has a strong influence on the propagation dynamics of the plume. With a smaller focal spot, the plume expansion is

[a)]Electronic mail: ssharilal@gmail.com. Present address: Prism Computational Sciences, Inc., 455 Science Drive, Madison, WI 53711.

found to be more spherical while with increasing spot size the plume is more directed normal to the target surface. The ion yield measurements with the Faraday cup also showed sharper decay in the ion flux with a larger spot size while narrower temporal ions profiles are noted with smaller spot sizes.

II. EXPERIMENTAL DETAILS

Details of the experimental setup are given elsewhere.[20] Briefly, for producing tin plasma, 1064 nm, 10 ns (full width at half maximum) pulses from a Nd: yttrium-aluminum-garnet laser was used. The target was placed in a stainless steel vacuum chamber that is pumped using a cryogenic pump and a base pressure of $\sim 10^{-6}$ Torr was easily maintained. The laser beam, at normal incidence, was focused onto the target using a planoconvex lens. The focal spot size at the target surface was measured using an optical imaging technique. A 2 mm thick tin target in the form of a slab was translated to provide a fresh surface for each shot to avoid errors associated with local heating and drilling.

Plume imaging was accomplished with an intensified charge coupled device (ICCD) camera placed orthogonal to the laser beam. A combination of lenses was used to image the plume region onto the camera to form a two-dimensional image of the plume intensity. A programmable timing generator was used to control the delay time between the laser pulse and the detector system with an overall temporal resolution of 1 ns. The visible radiation from the plasma was recorded integrally in a wavelength range of 350–900 nm.

The ion emission has been monitored using a Faraday cup (Kimball Physics) placed at a distance 15 cm from the target surface. The Faraday cup (FC) consists of an entrance aperture of 5 mm in diameter coupled to a cylindrical tube of diameter 1.3 cm. The collector plate is located 5 cm from the entrance aperture. For extracting positive ions, the FC is biased with a −30 V direct current voltage. The ion current is measured by acquiring the voltage signal across a load resistor by a 500 MHz digital phosphor oscilloscope.

III. RESULTS AND DISCUSSION

Fast photography that provides two-dimensional snap shots of the three-dimensional LPP propagation is one of the versatile diagnostic tools for understanding the expansion dynamics of laser created plumes.[21–25] This capability becomes essential for a hydrodynamic understanding of the plume propagation and reactive scattering. Plasma emission begins on the target surface soon after the laser photons reach the surface.[26] Images of the time evolution of the expanding tin plasma were taken in vacuum with different spot sizes. Typical ICCD images of the expanding plume at different times after the onset of plasma are given in Fig. 1 in vacuum. These images were recorded at a laser energy of 125 mJ and 60 μm spot size. The duration of the intensification (exposure time) varied from 2 to 20 ns and each image is obtained from a single laser pulse. Timing jitter is less than 1 ns. All images shown here have been normalized by the peak intensity in that image for better viewpoint.

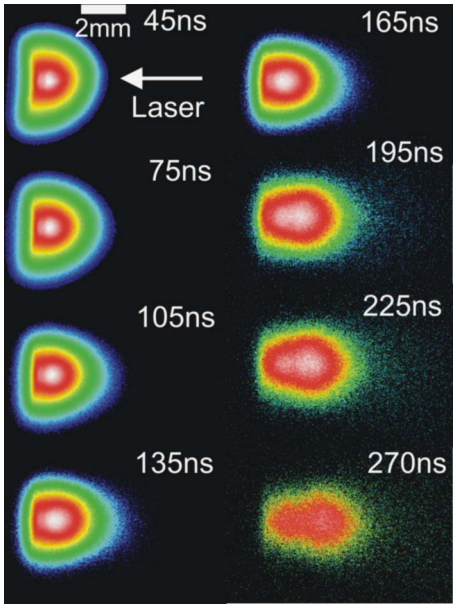

FIG. 1. (Color online) Images of the plume recorded with ICCD at different times after the onset of plasma formation in vacuum with 60 μm spot size. The time noted in the figures corresponds to the time after the onset of plasma formation. Each image is obtained from different laser shots and all the images are normalized to its maximum intensity and are shown in logarithmic scale for better clarity.

Plasma expansion into a vacuum environment is simply adiabatic and can be fully predicted by theoretical models and numerical gas dynamic simulations.[27] The three-dimensional plume propagation is governed by the initial pressure gradients and shape of the plume at the end of the laser pulse. We studied the expansion behavior of the plume with different spot sizes in vacuum using fast photography and noticed no difference in plume behavior. This is because plume species are not emitting at larger distances (>5 mm) as it expands freely in vacuum. In this context a partial pressure of ambient gas will be useful, since it makes plume more emitting due to efficient electron impact excitation and plasma recombination. Our previous studies showed that as the pressure increases from vacuum, there exists a transition regime, where the plume is characterized by a strong interpenetration of the plasma species and background gas that leads to plume splitting and sharpening.[10,20] During this stage of mutual penetration of the laser plasma and ambient gas, a considerable fraction of kinetic energy was converted into heat which in turn increases the temperature of the gas and radiation. The pressure range of the transition regime depends on several experimental parameters including, target mass, ambient gas mass, and laser intensity. In the present studies, with tin as a target and argon as an ambient we found the transition regime is around 300 mTorr. So we used an argon ambient pressure of 300 mTorr to make the plume more collisional.

Fast imaging in the transition region provides hydrodynamic properties of the plume. Images of the plume recorded with a 60 and 280 μm spot size are shown in Figs. 2 and 3, respectively. The images were recorded with 300 mTorr of argon pressure and 125 mJ of laser energy. Even though the images recorded in vacuum with 60 and 280 μm looked

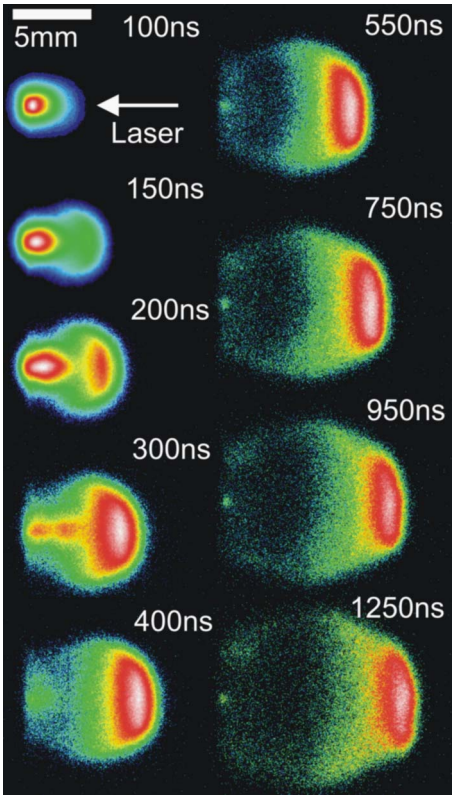

FIG. 2. (Color online) The plume images recorded with 60 μm spot size in the presence of 300 mTorr argon ambient. The times shown in the frames correspond to the time after the onset of plasma formation. Each shot is recorded with different laser shots and all images are normalized with its maximum intensity and are shown in logarithmic scale for better clarity.

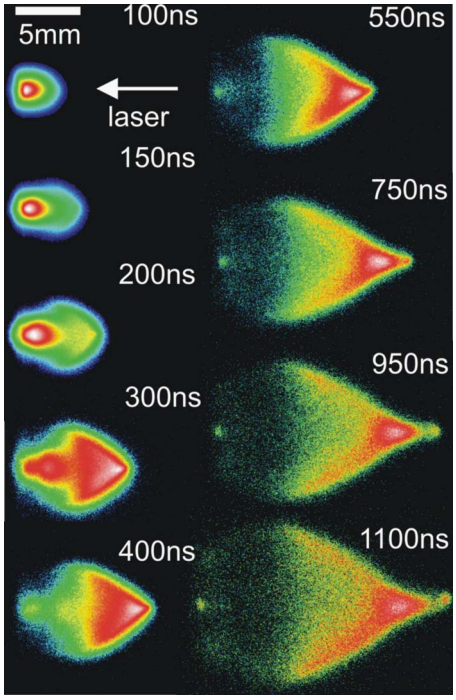

FIG. 3. (Color online) Images of the tin plume recorded with 280 μm spot size and 300 mTorr Ar pressure. The time shown in the figures indicates the time after the onset of plasma formation. All images are normalized to its maximum intensity and are shown in logarithmic scale for better clarity.

alike, the plume features showed dramatic variation when it expanded into an ambient partial pressure. The plume propagation changes significantly in the presence of a gas, especially at times >100 ns. The ambient gas has no influence on the plume propagation during the initial times of plasma expansion because the pressure of the plume is much higher than that of the ambient gas pressure. The plume expands rapidly until its driving pressure has deceased considerably, then a relatively sharp boundary is formed between the plume and background. The images show that the plume expansion is close to spherical geometry with 60 μm spot. With a larger spot size, the plume expansion is found to deviate from spherical expansion and a sharpening effect is observed. The shock region formed with 280 μm is more confined along the plume expansion axis (z axis) and is more arrow-head shaped similar to shock fronts often observed for projectiles, such as bullets traveling in air with supersonic velocities.

The presence of a background gas during LPP expansion can lead to the formation of stationary ambient plasma. This is caused by ionization of ambient gas atoms by prompt electrons and/or intense EUV light coming out from the early stages of plasma formation.[16,20] During initial times of plume expansion, the ablated species streams away from the target surface with supersonic free expansion. As time evolves, the plasma species start to sweep background gas species, leading to a pile of mass at the ablation front. This results in deceleration of the ablated plume and formation of a spherical shock wave. When a shock boundary is formed between the plume and ambient gas medium, it effectively shields the diffusion of the ambient gas species from the plasma species.

Emission intensity as function of distance along the direction of plume expansion is given in Fig. 4 for 60 and 280 μm spot sizes and at different times after the evolution of the plume. These plots are obtained from the ICCD images and provide useful information about the internal structures in the plume. For easier comparison, each profile has been normalized to its maximum intensity. The emission intensity profiles show single peak distribution at 100 ns after the onset of plasma formation indicating the absence of shock front formation. A weak shock region is observed in the plume front at 200 ns for both spot sizes as evidenced by the double peak structure in the emission profiles. The shock region intensity increases rapidly with time and at 300 ns, the emission from the shocked region is found to be much stronger compared to emission from other regions of the plasma. Also it is interesting to notice that at later times, especially after the strong shock formation, the time decay of the leading edge of the plume is getting much sharper than the trailing edge which is an indication of rapid deceleration of the plume front. An emission intensity peak feature is evident between the shock front and target with 300 ns profile and it could be caused by the scattering or reflection of the plume species in the backward direction from the shock region which interacts with incoming species.[9,28] This spatial splitting of the plume is entirely different from plume splitting observed previously using time of flight emission spectroscopy where a part of the plume species penetrated into the ambient region while the other part slowed down due to a collision with background gas.[10,12] This spatial splitting has

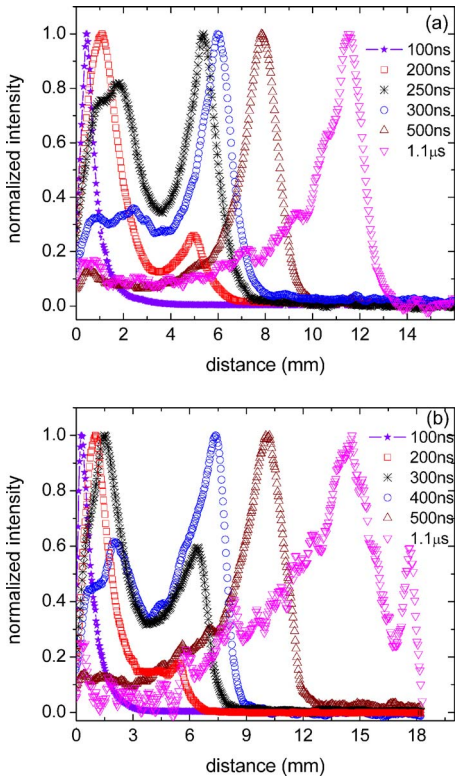

FIG. 4. (Color online) Intensity counts obtained from the ICCD images along the plume expansion direction (z axis) are given for various times after evolution of the plasma for (a) 60 and (b) 280 μm. For better comparison all the intensity profiles are normalized with respect to its maximum intensity.

been observed irrespective of the spot size used in the present studies. Plume splitting phenomena are evident in the images recorded with a 280 μm spot size at times greater than 1 μs where a part of the leading edge of the plume detached from the bulk region. It is worth it to note that similar plume splitting is absent with a smaller spot size.

As the images indicate, with a smaller spot size the plume expands spherically and a spherical shock wave model is a good approximation for the plume propagation. The position-time (R-t) plot obtained from the images is shown in Fig. 5. The R-t behavior of the shock wave is described by $R=\xi_0(E_0/\rho_0)^{1/5}t^{2/5}$, where ξ_0 is a constant related to specific heat capacity (γ), E_0 is the amount of energy released, and ρ_0 is the ambient gas density.[10] The solid line in Fig. 5 corresponding to the shock model fits well with the plume propagation with a smaller spot. The details of the plume slowing and shock wave formation have been studied thoroughly by several groups using theoretical and experimental methods.[5,9,10,29] The R-t plot obtained with a 280 μm spot showed a $t^{0.55}$ (dashed line in Fig. 5) dependence which clearly indicates deviation from the spherical shock expansion. These results show that the properties of shock front propagation are strongly dependent on the spot size and, hence, ablated mass. Shannon *et al.*[30] reported that the mass ablated during high power laser ablation varies nonlinearly with the spot size and laser power density which indeed affect the shock properties.

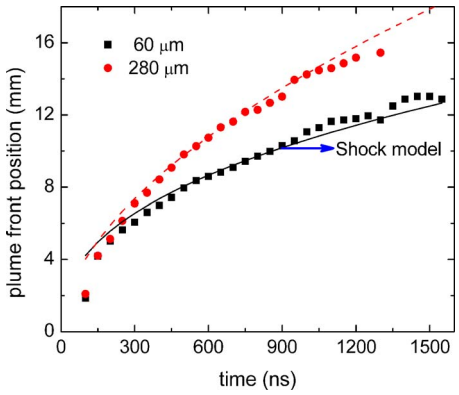

FIG. 5. (Color online) The plume front position as a function of the time delay obtained from the images for 60 and 280 μm spot sizes. The solid and dashed lines in the figure correspond to the $R\propto t^{0.4}$ and $t^{0.55}$ fit, respectively.

It is reported that tin plasma is optically thick to 13.5 nm radiation.[3,31] The interferometric analysis of tin plasma at an earlier time clearly showed the plasma scale length is shorter with a smaller spot size which leads to less reabsorption of 13.5 nm radiation. However, at the same time, higher lateral expansion can be expected with smaller spot sizes.[2,19] With a larger spot size, more EUV light can be generated due to high hydrodynamic coupling efficiency, but a longer plasma scale length results in heavier reabsorption and, hence, less EUV light can escape from the plasma. Hence, the final output of 13.5 nm EUV light with varying laser spot size is determined by the balance of the laser energy loss due to the lateral expansion and the reabsorption of EUV light which leads to constant CE irrespective of the laser spot size used. The present studies using fast photography of the tin plume confirm that the lateral expansion is higher with a smaller spot size and with increasing spot size plume elongation is higher.

We utilized a Faraday cup for measuring kinetic distributions of tin ions with different laser spot sizes. Faraday cups are routinely used for charge analysis in laser-produced plasmas. However, it should be remembered that space charge effects could distort the FC signal. Janmohamed *et al.*[32] reported a detailed description of the influence of space charge effects on the ion signal and they found that electrons play an important role in the space charge distortion phenomena. Typical time of flight (TOF) profiles recorded at the collector plate are given in Fig. 6 for tin ions in vacuum for 60 and 280 μm spot sizes. The velocity distribution obtained from the FC is also given in Fig. 6 as an inset. For collecting ions the FC is positioned at 15 cm away from the target surface and at an angle approximately 12 degrees with respect to the target normal. Since the presence of ambient partial pressure can slow down the fast moving ions,[16] the ion kinetic profiles recorded with the FC are done in vacuum. The ion TOF profile in vacuum is represented by a sharp prompt peak followed by a broad slower peak. The fast prompt peak in the ion signal is caused by the photoelectric effect and can be used as a time marker. It is evident from Fig. 6 that narrower current traces are produced by smaller spot sizes and these results are consistent with previous reports.[33] The broadening of the time of flight signal is mainly caused by an increase of slow particles in the tail of the FC signal. The estimated peak expansion velocity (v_p) of

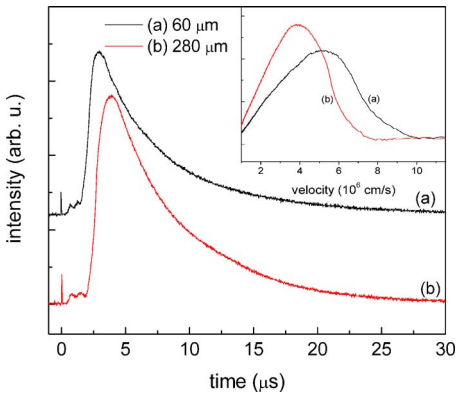

FIG. 6. (Color online) Typical ion signal recorded with a Faraday cup placed 15 cm from the target surface in vacuum for 60 and 280 μm spot sizes. The time of flight profiles are scaled vertically for a better view. The inset provides the velocity distribution obtained from the time of flight ion profiles.

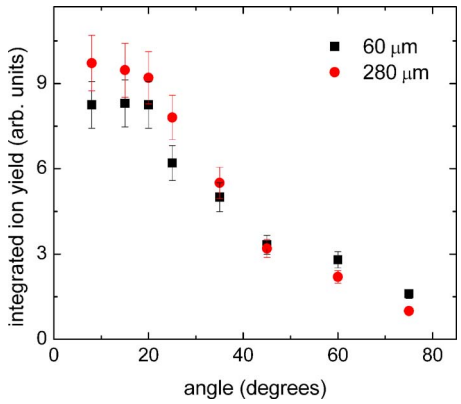

FIG. 7. (Color online) The angular distribution of ions recorded with a Faraday cup with 60 and 280 μm spot sizes.

positive ions is $\sim 4.9 \pm 0.4 \times 10^6$ cm s^{-1} for 60 μm and $3.7 \pm 0.4 \times 10^6$ for 280 μm spot diameters. The expansion velocity estimated from the FC is found to be greater than measured with ICCD plume images. Plume images recorded with an ICCD camera are spectrally integrated in the wavelength region 350–900 nm and in this spectral window, most of the emission from the Sn plasma is due to excited neutral and singly ionized tin.[34,35] But, it should be remembered that tin plasma contains highly charged Sn species and they are not emitting in the visible region. For example, the UTA emission around 13.5 nm is mainly contributed by Sn^{8+} to Sn^{13+} ions.[17]

In a laser-produced plasma, the velocity of the ions is dependent on their charge state and highly charged ions move with faster expansion velocity. This can be understood by considering the plume expansion in the initial stages where electrons strive to overtake the ions resulting in a space charge field that accelerates ions causing higher velocity for highly charged ionic states. The ions located at the front of the plasma acquire the largest energy during hydrodynamic acceleration and the interaction time for recombination is very much reduced.

Time of flight ion profiles showed narrower and faster kinetic energy distribution with a smaller spot size. Grun *et al.*[33] reported that the width of the ion velocity distributions from LPP depends strongly on the laser spot size and weakly on the laser intensity or plasma temperature. They also showed that the distribution width is governed by a scaling parameter, $r_s/c\tau$, where r_s is the laser focal spot radius at the target surface, c is the ion sound speed, and τ is the laser pulse width. The width to peak velocity ratio $(\Delta v/v_p)$ obtained from the FC signals showed values of 0.7 and 0.74 for 60 and 280 μm spot sizes, respectively. The estimated $r_s/c\tau$ values for these spot sizes are 0.1 and 0.45. Even though the scaling parameter agrees marginally with a larger spot size, a large discrepancy is observed with a smaller spot size. Gurn *et al.*[33] verified this scaling parameter for spot sizes from 200 μm to 1 mm. The discrepancy noticed in the scaling parameter may be caused by a smaller spot radius used in the present studies.

Figure 6 also shows the ion flux is higher with a larger spot size. It should be remembered that a change in the spot size can significantly influence the amount of ablated mass and, hence, the crater volume.[36] Depending on the laser irradiance and target material, mass removal can occur through desorption, thermal evaporation, exfoliation, phase explosion, and other mechanisms. The threshold for the occurrence of the earlier processes strongly depended on the laser wavelength and the laser spot size at the target surface. For example, Yoo *et al.*[36] reported the laser irradiance threshold for the phase explosion is roughly one order higher with 532 nm than 266 nm. They have not observed any rapid change in the crater volume with 1064 nm in the studied laser irradiance range $(1-10^3$ GW/cm$^2)$ and explained it is due to stronger plasma shielding and deeper optical penetration depth with the increasing wavelength. In LPP, the leading part of the laser pulse interacts with the target surface which leads to the formation of an energetic plume and the remaining part of the beam is utilized to heat up the plume. In other words, after the creation of the plasma, the target is screened off from the remaining part of the laser beam because of laser absorption by the plasma due to inverse bremsstrahlung.[37] The laser plasma interaction eventually heats up the plasma and more highly charged ions are produced. With a smaller spot size, the plasma scale length is smaller and the plume expands more spherically. With an increasing spot size, the plasma scale length becomes higher and the plasma expands more cylindrically. Hence, the coupling between the laser and plasma is higher with a larger spot size and the ions located in the front of the plume can gain more energy and accelerate.

The distribution of ions in a laser created plasma are best approximated by a single charge dependent Cos^n function where the value of n increases with the charge state and decreases with the atomic mass.[38] The ions of the highest ionization state dominate in the direction normal to the target, their concentration falls sharply away from the normal, and excited neutrals have the most angular spread. It can be due to the charge density at outer angular regions of the plume which is effectively diminished by recombination. Figure 7 provides the angular distribution of ion flux measured with the FC and it clearly shows the ion yield dropping rapidly away from the target normal. The Faraday cup is placed at a distance 15 cm from the target surface and the

total yield has been obtained by integrating the area under the ion profile. The ion flux is found to be higher for larger spot sizes at smaller angles with respect to the target normal and at larger angles the ion flux showed no difference with varying spot sizes. Figure 7 also indicates the plume ion distribution is much sharper with large spot size which agrees well with imaging studies.

IV. CONCLUSIONS

The spot size effects on the dynamics of the laser created tin plumes were investigated. For diagnosing the plume fast photography employing an ICCD and Faraday cup ion analysis were used. Although plume images looked alike at different spot sizes in vacuum, an addition of a partial argon pressure showed significant variation in the expansion dynamics of the plume especially at times later than 100 ns. Images showed the plume expands spherically with smaller spot sizes and the plume propagation is more cylindrical with larger spot sizes. Fast photography employing ICCD visible imaging also showed internal structures or spatial splitting of the plume irrespective of the laser spot sizes used. A sharpening and plume splitting phenomena is observed with a larger spot size. Faraday cup ion analysis indicated narrower and high velocity ion distribution with a smaller spot size. The ion flux estimate using the Faraday cup revealed that ion spreading is larger with a smaller spot size and that is consistent with plume imaging studies.

ACKNOWLEDGMENTS

The author thanks Dr. Mark Tillak, Dr. Yezeng Tao, and Dr. Beau O'Shay for fruitful discussions.

[1]V. Sizyuk, A. Hassanein, and T. Sizyuk, J. Appl. Phys. **100**, 103106 (2006).
[2]Y. Tao, M. S. Tillack, S. S. Harilal, K. L. Sequoia, and F. Najmabadi, J. Appl. Phys. **101**, 023305 (2007).
[3]S. Fujioka, H. Nishimura, K. Nishihara, A. Sasaki, A. Sunahara, T. Okuno, N. Ueda, T. Ando, Y. Z. Tao, Y. Shimada, K. Hashimoto, M. Yamaura, K. Shigemori, M. Nakai, K. Nagai, T. Norimatsu, T. Nishikawa, N. Miyanaga, Y. Izawa, and K. Mima, Phys. Rev. Lett. **95**, 235004 (2005).
[4]S. S. Harilal, M. S. Tillack, B. O'Shay, Y. Tao, R. Paguio, and A. Nikroo, Opt. Lett. **31**, 1549 (2006).
[5]D. B. Geohegan, in *Pulsed Laser Deposition of Thin Films*, edited by D. B. Chrisey and G. K. Hubler (Wiley, New York, 1994), p. 115.
[6]S. Arepalli, W. A. Holmes, P. Nikolaev, V. G. Hadjiev, and C. D. Scott, J. Nanosci. Nanotechnol. **4**, 762 (2004).
[7]A. Bailini, P. M. Ossi, and A. Rivolta, Appl. Surf. Sci. **253**, 7682 (2007).
[8]S. I. Anisimov, D. Bauerle, and B. S. Lukyanchuk, Phys. Rev. B **48**, 12076 (1993).
[9]S. Amoruso, A. Sambri, and X. Wang, J. Appl. Phys. **100**, 013302 (2006).
[10]S. S. Harilal, C. V. Bindhu, M. S. Tillack, F. Najmabadi, and A. C. Gaeris, J. Appl. Phys. **93**, 2380 (2003).
[11]J. Schou, in *Materials Surface Processing by Directed Energy Techniques*, edited by I. Pauleau (Elsevier, Amsterdam, 2006), p. 33.
[12]S. S. Harilal, C. V. Bindhu, M. S. Tillack, F. Najmabadi, and A. C. Gaeris, J. Phys. D **35**, 2935 (2002).
[13]S. Amoruso, R. Bruzzese, R. Velotta, N. Spinelli, M. Vitiello, and X. Wang, Appl. Surf. Sci. **248**, 45 (2005).
[14]R. F. Wood, K. R. Chen, J. N. Leboeuf, A. A. Puretzky, and D. B. Geohegan, Phys. Rev. Lett. **79**, 1571 (1997).
[15]M. Nieto, J. P. Allain, V. Titov, M. R. Hendricks, A. Hassanein, D. Rokusek, C. Chrobak, C. Tarrio, Y. Barad, S. Grantham, T. B. Lucatorto, and B. Rice, J. Appl. Phys. **100**, 053510 (2006).
[16]S. S. Harilal, B. O'Shay, Y. Tao, and M. S. Tillack, Appl. Phys. B: Lasers Opt. **86**, 547 (2007).
[17]S. S. Harilal, B. O'Shay, M. S. Tillack, Y. Tao, R. Paguio, A. Nikroo, and C. A. Back, J. Phys. D **39**, 484 (2006).
[18]S. S. Harilal, B. O'Shay, and M. S. Tillack, J. Appl. Phys. **98**, 036102 (2005).
[19]Y. Tao, S. S. Harilal, M. S. Tillack, B. O'Shay, and F. Najmabadi, Opt. Lett. **31**, 2492 (2006).
[20]S. S. Harilal, B. O'Shay, Y. Tao, and M. S. Tillack, J. Appl. Phys. **99**, 083303 (2006).
[21]S. Yalcin, Y. Y. Tsui, and R. Fedosejevs, IEEE Trans. Plasma Sci. **33**, 482 (2005).
[22]S. S. Harilal, B. O'Shay, M. S. Tillack, C. V. Bindhu, and F. Najmabadi, IEEE Trans. Plasma Sci. **33**, 474 (2005).
[23]G. Epurescu, J. Siegel, J. Gonzalo, F. J. Gordillo-Vazquez, and C. N. Afonso, Appl. Phys. Lett. **87**, 211501 (2005).
[24]H. Luna, K. D. Kavanagh, and J. T. Costello, J. Appl. Phys. **101**, 033302 (2007).
[25]S. S. Harilal, M. S. Tillack, B. O'Shay, C. V. Bindhu, and F. Najmabadi, Phys. Rev. E **69**, 026413 (2004).
[26]S. S. Harilal, C. V. Bindhu, and H. J. Kunze, J. Appl. Phys. **89**, 4737 (2001).
[27]M. W. Stapleton, A. P. McKiernan, and J. P. Mosnier, J. Appl. Phys. **97**, 064904 (2005).
[28]N. Arnold, J. Gruber, and J. Heitz, Appl. Phys. A: Mater. Sci. Process. **69**, S87 (1999).
[29]Z. Y. Chen, D. Bleiner, and A. Bogaerts, J. Appl. Phys. **99**, 063304 (2006).
[30]M. Shannon, A. X. Mao, A. Femandez, and R. E. Russo, Anal. Chem. **67**, 4522 (1995).
[31]J. J. MacFarlane, P. Wang, I. E. Golovkin, and P. R. Woodruff, Proc. SPIE **6151**, 61513Y (2006).
[32]R. Janmohamed, G. Redman, and Y. Y. Tsui, IEEE Trans. Plasma Sci. **34**, 455 (2006).
[33]J. Grun, R. Stellingwerf, and B. H. Ripin, Phys. Fluids **29**, 3390 (1986).
[34]S. S. Harilal, B. O'Shay, M. S. Tillack, and M. V. Mathew, J. Appl. Phys. **98**, 013306 (2005).
[35]M. V. Mathew, S. S. Harilal, and M. S. Tillack, J. Phys. D **40**, 447 (2007).
[36]J. H. Yoo, O. V. Borisov, X. Mao, and R. E. Russo, Anal. Chem. **73**, 2288 (2001).
[37]C. V. Bindhu, S. S. Harilal, M. S. Tillack, F. Najmabadi, and A. C. Gaeris, J. Appl. Phys. **94**, 7402 (2003).
[38]A. Thum-Jager and K. Rohr, J. Phys. D **32**, 2827 (1999).